

Slow-Down vs. Speed-Up of Diffusion in Non-Markovian Temporal Networks

Ingo Scholtes, Nicolas Wider, René Pfitzner, Antonios Garas,
Claudio Juan Tessone and Frank Schweitzer

Chair of Systems Design, ETH Zurich, Switzerland

www.sg.ethz.ch

Abstract

We study the slow-down and speed-up of diffusion in temporal networks with non-Markovian contact sequences. We introduce a causality-preserving time-aggregated representation that allows to analyze temporal networks from the perspective of spectral graph theory. With this we provide an analytical explanation for the frequently observed slow-down of diffusion in empirical non-Markovian temporal networks. We derive an analytical prediction for the magnitude of this slow-down and validate our prediction against two empirical data sets. Counterintuitively, we further show that non-Markovian properties can result in a speed-up of diffusion that can be related to the spectral properties of the underlying temporal network.

The evolution of dynamical processes in networks with time-varying topologies can deviate significantly from what one would expect from their corresponding static, time-aggregated representations. While the effects of node activity patterns, persistence and concurrency of interactions, as well as inter-event time distributions have been studied extensively [1, 2, 3, 4, 5, 6, 7, 8], non-Markovian properties in the contact sequences of temporal networks have been identified only recently as an independent mechanism that significantly affects dynamical processes [9, 10, 11, 12, 13, 14]. It has been shown that non-Markovian properties (i) alter the topology of causal interactions and (ii) slow-down diffusion processes in real-world temporal networks [11]. So far, an analytical explanation for this phenomenon, as well as for significant variations observed across different systems, is missing. To fill this gap, in this Letter we introduce an analytical approach to study diffusion dynamics in temporal networks with non-Markovian contact sequences. In particular, (i) we introduce higher-order time-aggregated representations of temporal networks that preserve causality, (ii) we show that spectral properties of these representations explain the slow-down of diffusion processes in temporal networks compared to aggregate networks, (iii) we show that non-Markovian properties can also result in a speed-up of diffusion, and (iv) we derive an analytical prediction for direction and magnitude of the change expected in a temporal network and validate it against empirical data.

We define a temporal network G^T to consist of directed, time-stamped edges $(v, w; t)$ for nodes v, w and discrete time stamps t . A (first-order) *aggregate network* $G^{(1)}$ can then be defined, where a directed edge (v, w) between nodes v and w exists whenever a time-stamped edge $(v, w; t)$

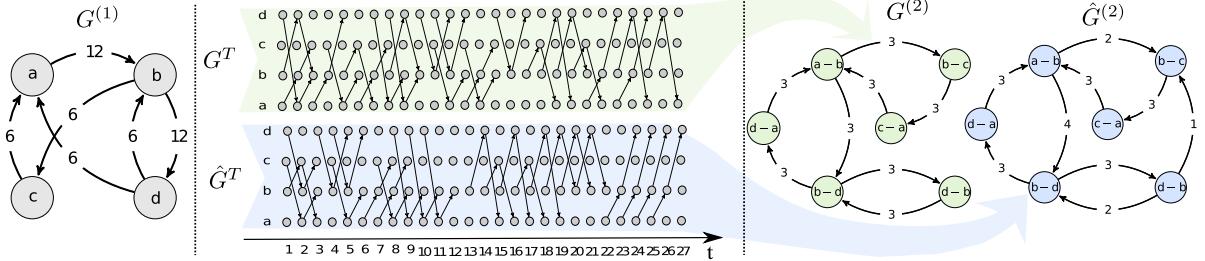


Figure 1: Two temporal networks G^T (top) and \hat{G}^T (bottom) giving rise to the same weighted, aggregate network $G^{(1)}$ (left panel). In the right panel, two second-order aggregate networks $G^{(2)}$ (left) and $\hat{G}^{(2)}$ (right) are shown that correspond to the two temporal networks G^T and \hat{G}^T . Both second-order aggregate networks are consistent with $G^{(1)}$.

exists in G^T for some time stamp t . In addition, edge weights $w^{(1)}(v, w)$ can be defined as the (relative) number of edge occurrences in the temporal network. A simple way to illustrate temporal networks are *time-unfolded* representations, in which time is unfolded into an additional topological dimension. In the resulting representation nodes v are replaced by temporal copies v_t for each time step t , while time-stamped edges $(v, w; t)$ are represented by edges (v_t, w_{t+1}) . In Fig. 1, time-unfolded representations of two different temporal networks (top, bottom) resulting in the same weighted aggregate network (left) are shown.

An important characteristic of temporal networks is that, compared to their corresponding time-aggregated representations, the *temporal transitivity* of paths does not necessarily hold. By this, we mean that a *path* $(a, b) \rightarrow (b, c)$ in a time-aggregated network does not imply that a and c are connected via a *time-respecting path* in the underlying temporal network [9, 15]. A time-respecting path connecting a and c only exists if the edge $(a, b; t)$ occurs *before* $(b, c; t')$, i.e. $t < t'$. Hence, the order of interactions in temporal networks affects the topology of time-respecting paths - and thus causality - in dynamic complex systems. A particularly simple way to study causality in temporal networks is in terms of the statistics of time-respecting paths of length two, so-called *two-paths* consisting of edges $(a, b; t) \rightarrow (b, c; t')$ for $t < t'$. Recent studies on the statistics of two-paths revealed that - compared to what one expects from a weighted time-aggregated network - nodes often preferentially mediate information flows between particular pairs of their neighbors, a phenomenon termed *betweenness preference* [11]. Thus, such temporal networks have non-Markovian characteristics, since the next contact in a contact sequence depends not only on the current, but also on the previous one. This characteristic is present in real-world systems and significantly changes dynamical processes [11, 12, 13].

In this Letter, we study the effect of these correlations on diffusion dynamics in temporal networks. In particular, we utilize a random walk process and study the time needed until node visitation probabilities converge to a stationary state [16, 17]. This convergence behavior of a

random walk is a simple proxy that captures the influence of both the topology and dynamics of temporal networks on general diffusive processes [18]. A standard approach to assess the convergence behavior of random walks is to study the evolution of the *total variation distance* between observed node visitation probabilities and the stationary distribution [19]. For a distribution π_k of visitation probabilities of nodes v after k steps of a random walk and a stationary distribution π , the total variation distance is defined as $\Delta(\pi_k, \pi) := \frac{1}{2} \sum_v |\pi(v) - \pi_k(v)|$. The convergence time $t(\epsilon)$ of a random walk can then be defined as the minimum number of steps k after which $\Delta(\pi_k, \pi)$ falls below a given threshold distance ϵ .

To illustrate the effect of non-Markovian properties, we study random walk convergence for three empirical temporal networks: (AN) time-stamped interactions in ant colonies [20]; (RM) time-stamped social interactions between students and academic staff [21]; and (FL) time-ordered flight itineraries passing through airports in the US ¹. We compute *average* convergence times $t_{agg}(\epsilon)$ and $t_{temp}(\epsilon)$ after which the total variation distance of a random walk falls below a threshold ϵ in (i) the weighted aggregated network and (ii) a temporal network model derived from the empirical contact sequence respectively. To focus on non-Markovian properties and exclude effects of inter-event time distributions, this model only preserves the weighted aggregate network as well as the statistics of two-paths in the data. For some threshold ϵ we define a slow-down factor $\mathcal{S}(\epsilon) := t_{temp}(\epsilon)/t_{agg}(\epsilon)$ capturing the change of diffusive behavior in the temporal compared to the aggregate network. Fig. 2 shows the slow-down for the three empirical networks and different convergence thresholds ϵ . Even though networks are of comparable size ², deviations from the corresponding aggregate networks in the limit of small ϵ are very different. For $\epsilon = 10^{-5}$ and (RM) the slow-down factor is $\mathcal{S} \approx 8.63 \pm 0.01$, while for (AN) it is $\mathcal{S} \approx 2.21 \pm 0.02$. For (FL), we obtain $\mathcal{S} \approx 0.957 \pm 0.002$, indicating a speed-up of convergence compared to the aggregate network.

In the following we provide an analytical explanation for the direction of this change (i.e. slow-down or speed-up) as well as for its magnitude in specific temporal networks. In particular, we show that spectral properties of higher-order, time-aggregated networks allow to calculate an analytical estimate \mathcal{S}^* for the slow-down \mathcal{S} observed in empirical temporal networks. Our approach utilizes a *state space expansion* to obtain a higher-order Markovian representation of non-Markovian temporal networks. This means that a non-Markovian *sequence of interactions* in which the next interaction only depends on the previous one (i.e. one-step memory), can be modeled by a Markovian stochastic process that generates a *sequence of two-paths*. For this, we define a *second-order aggregate network* $G^{(2)} = (V^{(2)}, E^{(2)})$ in which each node $e \in V^{(2)}$ represents an edge in the first-order aggregate network $G^{(1)}$. As edges $E^{(2)}$, we define all possible

¹We use a 10 % sample of airline tickets sold in the USA, freely available via the RITA TranStats Airline Origin and Destination Survey (DB1B) database http://www.transtats.bts.gov/Tables.asp?DB_ID=125. For our study we extracted 230,000 transit flights ticketed by American Airlines in the fourth quarter of 2001.

²Empirical temporal networks consist of 61 (AN), 58 (RM), and 116 (FL) nodes.

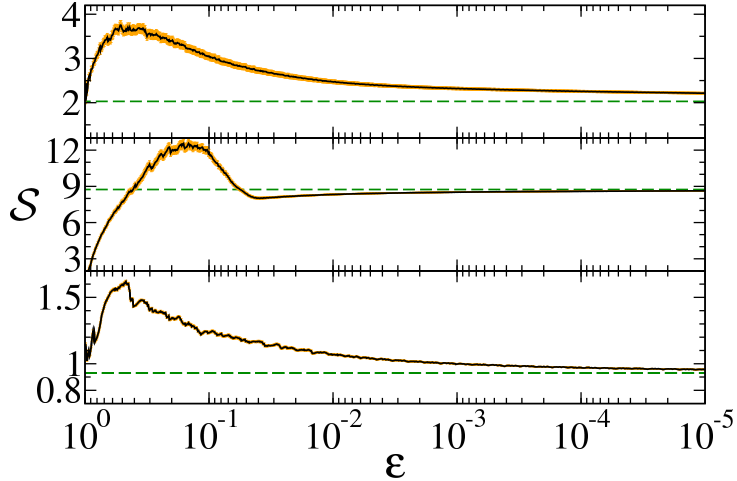


Figure 2: Slow-down factor $\mathcal{S}(\epsilon)$ of convergence time of random walks with convergence threshold ϵ in temporal networks generated by (i) a model preserving two-path statistics compared to (ii) a random walk in the weighted time-aggregated network for the (AN) (top), (RM) (middle) and (FL) dataset (bottom). Results are averages over all starting nodes, error bars indicate the standard error. The predicted \mathcal{S}^* value (see Eq. 6) is shown by the horizontal dashed line.

paths of length two in $G^{(1)}$, i.e. the set of all pairs (e_1, e_2) for edges $e_1 = (a, b)$ and $e_2 = (b, c)$ in $G^{(1)}$. Based on a temporal network G^T , weights $w^{(2)}(e_1, e_2)$ in the second-order network are defined based on the frequency of two-paths $(a, b; t-1) \rightarrow (b, c; t)$ in G^T , while proportionally correcting for multiple two-paths $(a', b; t-1) \rightarrow (b, c'; t)$ passing through node b at the same time. We define ³

$$w^{(2)}(e_1, e_2) := \sum_t \frac{\delta_{(a,b;t-1)} \delta_{(b,c;t)}}{\sum_{a',c' \in V} \delta_{(a',b;t-1)} \delta_{(b,c';t)}}, \quad (1)$$

where $\delta_{(a,b;t)} = 1$ if edge $(a, b; t)$ exists in the temporal network G^T and $\delta_{(a,b;t)} = 0$ otherwise. By this construction we obtain a *second-order aggregate network* $G^{(2)}$ where (i) each node represents an edge in the underlying temporal network, (ii) each edge represents a two-path, and (iii) weights $w^{(2)}$ capture the statistics of two-paths in the temporal network. Two second-order aggregate networks $G^{(2)}$ and $\hat{G}^{(2)}$ with weights corresponding to the example networks G^T and \hat{G}^T are depicted in the right panel of Fig. 1. This construction allows to define a second-order Markov model generating contact sequences exhibiting “one-step memory” and thus reproducing the statistics of two-paths. For two-paths $e_1 \rightarrow e_2$ we define entries of a transition matrix $\mathbf{T}^{(2)}$ for a

³This definition considers two-paths consisting of directly consecutive edge activations. It is simple to generalize weights to capture two-paths $(a, b; t') - (b, c, t)$ for $1 \leq t - t' \leq \epsilon$

random walk in $G^{(2)}$ with weights $w^{(2)}$ as

$$T_{e_1 e_2}^{(2)} := w^{(2)}(e_1, e_2) \left(\sum_{e' \in V^{(2)}} w^{(2)}(e_1, e') \right)^{-1}. \quad (2)$$

If $\mathbf{T}^{(2)}$ is primitive, the Perron-Frobenius theorem guarantees that a unique leading eigenvector π of $\mathbf{T}^{(2)}$ exists⁴. This eigenvector captures the stationary activation frequencies of edges in contact sequences generated by a random walk with transition matrix $\mathbf{T}^{(2)}$ (examples corresponding to temporal networks shown in Fig. 1 are provided in supplementary material).

Interpreting $\mathbf{T}^{(2)}$ as transition matrix of a random walker in $G^{(2)}$, we obtain a second-order Markov model generating contact sequences that preserve (i) the weights in the first-order aggregate network, and (ii) the statistics of two-paths. In line with recent observations that one-step memory is often sufficient to characterize time-respecting paths in empirical temporal networks [13], in the remainder of this Letter we focus on such second-order models. However, our findings can be generalized to n -th order networks $G^{(n)}$ and matrices $\mathbf{T}^{(n)}$ that capture the statistics of time-respecting paths of length n . From this perspective, the weighted aggregate network $G^{(1)}$ can be seen as a first-order approximation where weights $w^{(1)}$ capture the statistics of paths of length one. Contact sequences generated by a random walk in $G^{(1)}$ with transition probabilities proportional to edge weights $w^{(1)}$ preserve the statistics of edges but destroy the statistics of two-paths. As such, a random walk in $G^{(1)}$ represents a null model that changes the statistics of time-respecting paths and thus alters causality in temporal networks. The same null model can be defined based on $G^{(2)}$ by constructing a maximum entropy transition matrix $\tilde{\mathbf{T}}^{(2)}$ which (i) preserves the weights $w^{(1)}$ of edges in $G^{(1)}$ and (ii) creates ‘‘Markovian’’ temporal networks. For $e_1 = (a, b)$ and $e_2 = (b, c)$, the entries $\tilde{T}_{e_1 e_2}^{(2)}$ corresponding to a two-path $e_1 \rightarrow e_2$ are given as

$$\tilde{T}_{e_1 e_2}^{(2)} := w^{(1)}(b, c) \left(\sum_{c' \in V^{(1)}} w^{(1)}(b, c') \right)^{-1}. \quad (3)$$

Each transition matrix $\mathbf{T}^{(2)}$ whose leading eigenvector π satisfies $\pi_e = w^{(1)}(a, b)$ (\forall edges $e = (a, b)$) defines a statistical ensemble of temporal networks constrained by a weighted time-aggregated network $G^{(1)}$ and a given two-path statistics. The entropy of this ensemble can be defined based on the entropy growth rate of $\mathbf{T}^{(2)}$ as

$$H(\mathbf{T}^{(2)}) := - \sum_{e \in E^{(1)}} \pi_e \sum_{e' \in E^{(1)}} T_{ee'}^{(2)} \log_2 \left(T_{ee'}^{(2)} \right). \quad (4)$$

⁴ $\mathbf{T}^{(2)}$ can always be made primitive by restricting it to the largest strongly connected component of $G^{(2)}$ and adding small positive diagonal entries.

Different from entropy measures previously applied to dynamic networks [22], this measure quantifies to what extent the next step in a contact sequence is determined by the previous contact. For a transition matrix $\mathbf{T}^{(2)}$, the ratio of entropy growth between $\mathbf{T}^{(2)}$ and the (maximum entropy) model $\tilde{\mathbf{T}}^{(2)}$ can be given as

$$\Lambda_H(\mathbf{T}^{(2)}) := H(\mathbf{T}^{(2)})/H(\tilde{\mathbf{T}}^{(2)}). \quad (5)$$

This ratio ranges between 0 for transition matrices generating deterministic contact sequences and 1 for the case $\tilde{\mathbf{T}}^{(2)}$ representing Markovian temporal networks. A value of $\Lambda_H(\mathbf{T}^{(2)}) < 1$ highlights that the statistics of two-paths deviates from what is expected based on the first-order aggregate network. As such, Λ_H is a simple measure capturing the importance of non-Markovian properties in temporal networks.

Diffusion in Temporal Networks. An interesting aspect of the second-order representation $G^{(2)}$ is that temporal transitivity holds, i.e. the existence of edges (e_1, e_2) and (e_2, e_3) in $G^{(2)}$ implies that a time-respecting path $e_1 \rightarrow e_2 \rightarrow e_3$ exists in the temporal network G^T ⁵. This enables the use of algebraic methods and hence to relate diffusion dynamics in temporal networks with spectral properties of the matrix $\mathbf{T}^{(2)}$. In particular, the convergence time of random walks is related to the second largest eigenvalue of its transition matrix. For a primitive stochastic matrix with (not necessarily real) eigenvalues $1 = \lambda_1 > |\lambda_2| > |\lambda_3| \geq \dots \geq |\lambda_n|$, one can show that the number of steps k after which the total variation distance $\Delta(\pi_k, \pi)$ between the visitation probabilities π_k and the stationary distribution π of a random walk falls below ϵ is proportional to $1/\ln(|\lambda_2|)$ (see supplementary material included in this article for a detailed derivation). For a matrix $\mathbf{T}^{(2)}$ capturing the statistics of two-paths in an empirical temporal network (see Eq. 2), and a matrix $\tilde{\mathbf{T}}^{(2)}$ representing the ‘‘Markovian’’ model derived from the aggregate network $G^{(1)}$ (see Eq. 3), an analytical prediction \mathcal{S}^* for the change of convergence speed that is due to non-Markovian properties can be derived as

$$\mathcal{S}^*(\mathbf{T}^{(2)}) := \ln(|\tilde{\lambda}_2|)/\ln(|\lambda_2|), \quad (6)$$

where λ_2 and $\tilde{\lambda}_2$ denote the second largest eigenvalue of $\mathbf{T}^{(2)}$ and $\tilde{\mathbf{T}}^{(2)}$ respectively. Depending on λ_2 and $\tilde{\lambda}_2$ a slow-down ($\mathcal{S}^*(\mathbf{T}^{(2)}) > 1$) or speed-up ($\mathcal{S}^*(\mathbf{T}^{(2)}) < 1$) of diffusion can occur.

Data Analysis. Based on this approach, we analytically study the effect of non-Markovian characteristics in the empirical networks introduced above. For each data set we construct matrices $\mathbf{T}^{(2)}$ and $\tilde{\mathbf{T}}^{(2)}$ as defined in Eqs. 2 and 3, and we compute the entropy growth rate ratio

⁵Notably, the same is not true for the first-order representation $G^{(1)}$, since *temporal transitivity* does not necessarily hold in terms of time-respecting paths; i.e. the existence of edges (a, b) and (b, c) in $G^{(1)}$ does not imply that a time-respecting path $a \rightarrow b \rightarrow c$ exists.

Λ_H for the corresponding statistical ensembles. For (RM) we obtain $\Lambda_H(\mathbf{T}^{(2)}) \approx 0.39$ and for (AN) $\Lambda_H(\mathbf{T}^{(2)}) \approx 0.43$, while for (FL) $\Lambda_H(\mathbf{T}^{(2)}) \approx 0.82$. This indicates that the topologies of time-respecting paths in all three cases differ from what is expected from the first-order aggregate networks. The impact of these differences on diffusion can be quantified by means of the analytical prediction $\mathcal{S}^*(\mathbf{T}^{(2)})$: For (RM) we obtain $\mathcal{S}^*(\mathbf{T}^{(2)}) \approx 8.74$ and for (AN) $\mathcal{S}^*(\mathbf{T}^{(2)}) \approx 2.03$, while for (FL) $\mathcal{S}^*(\mathbf{T}^{(2)}) \approx 0.93$. These predictions are consistent with the behavior observed in numerical simulations in the limit of small ϵ (see Fig. 2). The significantly smaller magnitude of the slow-down \mathcal{S} in (AN) compared to (RM) can neither be attributed to differences in system size nor inter-event time distribution (which are removed by our model). A spectral analysis of $\mathbf{T}^{(2)}$ can explain the smaller slow-down of (AN) compared to (RM) by a “better connected” causal topology indicated by a smaller \mathcal{S}^* . For (FL), the analytical prediction $\mathcal{S}^*(\mathbf{T}^{(2)}) \approx 0.93$ is consistent with the asymptotic empirical speed-up observed in Fig. 2. The non-linear behavior of $\mathcal{S}(\epsilon)$ can be understood by recalling that Eq. 6 assumes that only λ_2 contributes to the convergence time, which holds in the limit of small ϵ . As ϵ increases, an increasing number of eigenvalues and eigenvectors have non-negligible contributions to the empirical slow-down \mathcal{S} .

In order to highlight a simple mechanism that can give rise to both a slow-down or speed-up of diffusion, we introduce the following toy model. The model generates non-Markovian temporal networks consistent with a uniformly weighted aggregate network with two interconnected communities, each consisting of a random 4-regular graph with 50 nodes. A parameter $\sigma \in (-1, 1)$ controls whether two-paths between nodes in *different* communities are - compared to a “Markovian” realization - over- ($\sigma > 0$) or under-represented ($\sigma < 0$). The Markovian case coincides with $\sigma = 0$. Realizations generated for any parameter σ are consistent with the same weighted aggregate network (see supplementary material included in this article for model details). Fig. S3 shows the effect of σ on the entropy growth rate ratio Λ_H (blue, dashed line) and the predicted slow-down \mathcal{S}^* (black, solid line). All non-Markovian realizations of the model (i.e. $\sigma \neq 0$) exhibit an entropy growth rate ratio $\Lambda_H < 1$. Whether this results in a speed-up ($\mathcal{S}^* < 1$) or slow-down ($\mathcal{S}^* > 1$) depends on how order correlations are aligned with community structures. For $\sigma < 0$, time-respecting paths across communities are *inhibited* and diffusion slows down compared to the aggregate network ($\mathcal{S}^*(\mathbf{T}^{(2)}) > 1$). For $\sigma > 0$, non-Markovian properties *enforce* time-respecting paths across communities and thus *mitigate the decelerating effect of community structures* on diffusion dynamics ($\mathcal{S}^*(\mathbf{T}^{(2)}) < 1$) [23]. This intuitive interpretation can be substantiated by a spectral analysis (see supplementary material included in this article).

In summary, we introduce second-order aggregate representations of non-Markovian temporal networks. This abstraction allows to define Markov models generating statistical ensembles of temporal networks that preserve (i) the weighted aggregate network and (ii) the statistics of time-respecting paths of length two (see Eq. 2). A transition matrix for this model can easily be computed based on empirical contact sequences. The ratio of entropy growth (see Eq. 5)

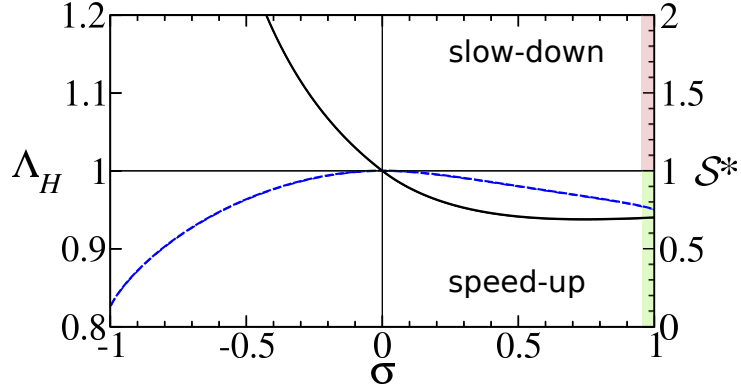


Figure 3: Entropy growth rate ratio Λ_H (blue, dashed line) and slow-down factor \mathcal{S}^* (black, solid line) for a model of non-Markovian temporal networks which are consistent with a weighted aggregate network that shows two pronounced communities. A parameter σ controls whether two-paths across communities are over-represented ($\sigma > 0$) or under-represented ($\sigma < 0$) compared to the Markovian case ($\sigma = 0$).

between this transition matrix and that of a null model generated from a first-order aggregate network allows to assess the importance of non-Markovian properties in temporal networks. We show that spectral properties of the transition matrices capture the connectivity of the causal topology of temporal networks and allow to predict (i) whether non-Markovian properties slow-down or speed-up random walk convergence and (ii) the magnitude of this change (see Eq. 6). With this, we provide one of the first analytical explanations for changes in diffusion dynamics observed in empirical temporal networks. Finally, we argue that the higher-order aggregate networks introduced in this Letter are simple static representations of temporal networks which - in contrast to first-order aggregate networks - preserve causality. This approach provides interesting perspectives for (i) temporal community detection by spectral clustering, (ii) refined centrality measures in dynamic networks, and (iii) analytical studies of dynamical processes in complex systems with time-varying interaction topologies.

Acknowledgements. We acknowledge feedback by R. Burkholz on the manuscript. I.S. and R.P. acknowledge support by SNF project CR_3111_140644. N.W., A.G. and F.S. acknowledge support by EU-FET project MULTIPLEX 317532.

Supplementary Material

This supplementary material contains illustrative examples, technical details about the derivation of the slow-down factor \mathcal{S}^* as well as details about a model for non-Markovian temporal networks that can be parameterized to produce temporal networks that slow-down or speed-up diffusion. We further include a spectral analysis of second-order aggregate networks that substantiate our interpretation that temporal correlations can mitigate the decelerating effect of communities on diffusion dynamics.

Illustrative Examples In our Letter, we introduce matrices $\mathbf{T}^{(2)}$ (Eq. 2 in the Letter) and $\tilde{\mathbf{T}}^{(2)}$ (Eq. 3 in the Letter) representing a second-order Markov model for interaction sequences in temporal networks with one-step memory. For the temporal network example G^T shown in Fig. 1 (middle-top) of our Letter and its second-order aggregate network $G^{(2)}$ shown in Fig. 1 (right panel), $\mathbf{T}^{(2)}$ (rows/columns ordered as indicated) is given as

$$\mathbf{T}^{(2)} = \begin{array}{l} (a, b) \\ (b, c) \\ (b, d) \\ (c, a) \\ (d, a) \\ (d, b) \end{array} \left| \begin{array}{cccccc} \left(\begin{array}{cccccc} 0 & 1/2 & 1/2 & 0 & 0 & 0 \\ 0 & 0 & 0 & 1 & 0 & 0 \\ 0 & 0 & 0 & 0 & 1/2 & 1/2 \\ 1 & 0 & 0 & 0 & 0 & 0 \\ 1 & 0 & 0 & 0 & 0 & 0 \\ 0 & 0 & 1 & 0 & 0 & 0 \end{array} \right) \end{array} \right.$$

As normalized leading eigenvector π of $\mathbf{T}^{(2)}$ we obtain $\pi = (\frac{1}{4}, \frac{1}{8}, \frac{1}{4}, \frac{1}{8}, \frac{1}{8}, \frac{1}{8})$. The leading eigenvector π captures the stationary activation frequencies of edges and thus corresponds to the relative weights of edges in the network $G^{(1)}$ (see relative weights of $G^{(1)}$ shown in Fig. 1 (left panel) of the Letter). Based on a weighted first-order aggregate network $G^{(1)}$, in Eq. 3 of our Letter we further introduce a matrix $\tilde{\mathbf{T}}^{(2)}$ that corresponds to a ‘‘Markovian’’ temporal network consistent with $G^{(1)}$. For the example $G^{(1)}$ shown in Fig. 1 of our Letter, $\tilde{\mathbf{T}}^{(2)}$ is given as

$$\tilde{\mathbf{T}}^{(2)} = \begin{array}{l} (a, b) \\ (b, c) \\ (b, d) \\ (c, a) \\ (d, a) \\ (d, b) \end{array} \left| \begin{array}{cccccc} \left(\begin{array}{cccccc} 0 & 1/3 & 2/3 & 0 & 0 & 0 \\ 0 & 0 & 0 & 1 & 0 & 0 \\ 0 & 0 & 0 & 0 & 1/2 & 1/2 \\ 1 & 0 & 0 & 0 & 0 & 0 \\ 1 & 0 & 0 & 0 & 0 & 0 \\ 0 & 1/3 & 2/3 & 0 & 0 & 0 \end{array} \right) \end{array} \right.$$

Again, as leading eigenvector of $\tilde{\mathbf{T}}^{(2)}$ we obtain $\pi = (\frac{1}{4}, \frac{1}{8}, \frac{1}{4}, \frac{1}{8}, \frac{1}{8}, \frac{1}{8})$, confirming that the stationary activation frequencies of edges in the temporal network ensembles $\tilde{\mathbf{T}}^{(2)}$ and $\mathbf{T}^{(2)}$ are the same. This confirms that temporal networks generated by $\mathbf{T}^{(2)}$ and $\tilde{\mathbf{T}}^{(2)}$ are consistent with the same weighted aggregate network $G^{(1)}$.

The fact that $\mathbf{T}^{(2)}$ corresponds to non-Markovian temporal networks can be confirmed by computing the entropy growth rate ratio $\Lambda_H(\mathbf{T}^{(2)})$ (see Eqs. 4 and 5 in our Letter). For the matrices $\mathbf{T}^{(2)}$ and $\tilde{\mathbf{T}}^{(2)}$ we obtain $\Lambda_H(\mathbf{T}^{(2)}) = 0.84$ and thus $\Lambda_H(\mathbf{T}^{(2)}) < 1$.

Derivation of Slow-Down Factor In our Letter, we argue that changes of diffusion dynamics in temporal networks as compared to their static counterparts, are due to the change of *connect- edness* or *conductance* of the corresponding *second-order aggregate network*. We further show that these changes are captured by a slow-down factor which can be computed based on the second-order aggregate networks corresponding to a particular non-Markovian temporal network and its Markovian counterpart. In the following, we substantiate our approach by analytical arguments, highlighting the conditions under which our prediction is accurate.

For a second-order aggregate network $G^{(2)}$ with a weight function $w^{(2)}$, let us consider a transition matrix $\mathbf{T}^{(2)}$ as defined in Eq. 2 of our Letter. The influence of the eigenvalues of $\mathbf{T}^{(2)}$ on the convergence behavior of a random walk can then be studied as follows. For a sequence of eigenvalues $1 = \lambda_1 \geq |\lambda_2| \geq \dots \geq |\lambda_n|$ of $\mathbf{T}^{(2)}$ with corresponding eigenvectors v_1, \dots, v_n , we define the *eigen- matrix* $\mathbf{U} := (v_i)_{i=1, \dots, n}$. We further define a stochastic row vector $x = \pi_0 = (p_1, \dots, p_n)$ which we assume contains the initial node visitation probabilities before the random walk starts. Since \mathbf{U} is not necessarily regular (n.b. that $G^{(2)}$ is directed) we use a Moore-Penrose pseudoinverse [24] \mathbf{U}^{-1} of \mathbf{U} as well as diagonal matrix $\mathbf{D} = \text{diag}(\lambda_1, \dots, \lambda_n)$ to obtain an eigendecomposition of $\mathbf{T}^{(2)}$ as

$$\mathbf{T}^{(2)} = \mathbf{U}^{-1} \mathbf{D} \mathbf{U}. \quad (\text{S1})$$

We can then transform the vector x into an eigenspace representation of $\mathbf{T}^{(2)}$ and obtain $a = x \mathbf{U}^{-1}$ such that $x = \sum_{i=1}^n a_i v_i$. With this, the node visitation probability vector π_k after k steps can be expressed as

$$\pi_k = x \mathbf{T}^k = \sum_{i=1}^n a_i v_i \mathbf{T}^k$$

Repeated substitution according to the eigenvalue equation $v_i \mathbf{T} = \lambda_i v_i$ yields

$$\pi_k = \sum_{i=1}^n \lambda_i^k a_i v_i.$$

Assuming that $\mathbf{T}^{(2)}$ is primitive, for the Perron-Frobenius eigenvalue λ_1 we obtain $1 = \lambda_1 > |\lambda_2|$ and the normalized first eigenvector $a_1 v_1$ corresponds to the unique stationary distribution $\pi = \pi_k$ of the Markov chain given by $\mathbf{T}^{(2)}$. For the first term in the sum above, we thus obtain $\lambda_1^k a_1 v_1 = 1 \cdot \pi = \pi$. With

$$\pi_k = \pi + \sum_{i=2}^n \lambda_i^k a_i v_i \quad (\text{S2})$$

a difference vector $\delta(k)$ whose components $\delta_j(k)$ capture the difference between node visitation probabilities $\pi_k(j)$ and the stationary distribution $\pi(j)$ for each node j after k steps of the random walk can be defined as

$$\delta(k) = \pi_k - \pi = \sum_{i=2}^n \lambda_i^k a_i v_i. \quad (\text{S3})$$

The total variation distance

$$\Delta(\pi_k, \pi) := \frac{1}{2} \sum_{j=1}^n |\pi(j) - \pi_k(j)|$$

after k steps can then be given as

$$\begin{aligned} \Delta(\pi_k, \pi) &= \frac{1}{2} \sum_{j=1}^n |\delta_j(k)| \\ &= \frac{1}{2} \sum_{j=1}^n |\lambda_2^k a_2 (v_2)_j + \lambda_3^k a_3 (v_3)_j \\ &\quad + \dots + \lambda_n^k a_n (v_n)_j| \end{aligned}$$

where $(v_i)_j$ denotes the j -th component of eigenvector v_i . Under the condition that $|\lambda_2|$ is not degenerate (i.e. $|\lambda_2| > |\lambda_3|$) and using the fact that $|\lambda_i| < 1$ for $i \geq 2$ (n.b. that $\mathbf{T}^{(2)}$ is primitive and thus $G^{(2)}$ is necessarily strongly connected) for k sufficiently large one can make the following approximation:

$$\Delta(\pi_k, \pi) \approx \frac{1}{2} \sum_{j=1}^n |\lambda_2^k a_2 (v_2)_j|.$$

For a sufficiently small convergence threshold $\epsilon > 0$, the convergence time k after which the total variation distance falls below ϵ can then be calculated as follows:

$$\begin{aligned} \Delta(\pi_k, \pi) &\approx \frac{1}{2} \sum_{j=1}^n |\lambda_2^k a_2 (v_2)_j| \leq \epsilon \Leftrightarrow \\ k \cdot \ln(|\lambda_2|) + \ln \left(\frac{1}{2} \sum_{j=1}^n |a_2 (v_2)_j| \right) &\leq \ln(\epsilon) \Leftrightarrow \\ k &\geq \frac{1}{\ln(|\lambda_2|)} \cdot \left(\ln(\epsilon) - \ln \left(\frac{1}{2} \sum_{j=1}^n |a_2 (v_2)_j| \right) \right) \end{aligned}$$

Here, we utilize the fact that, since $|\lambda_2| > |\lambda_3|$, both λ_2 and $a_2 v_2$ are necessarily real and thus $|\lambda_2^k a_2(v_2)_j| = |\lambda_2^k| \cdot |a_2(v_2)_j| = |\lambda_2|^k \cdot |a_2(v_2)_j|$. Based on the result above, the convergence time $t(\epsilon)$ after which total variation falls below ϵ (i.e. $\forall k \geq t(\epsilon) : \Delta(\pi_k, \pi) \leq \epsilon$) is then given as

$$t(\epsilon) = \frac{1}{\ln(|\lambda_2|)} \cdot \left(\ln(\epsilon) - \ln \left(\frac{1}{2} \sum_{j=1}^n |a_2(v_2)_j| \right) \right).$$

We now consider the null model $\tilde{\mathbf{T}}^{(2)}$ corresponding to a Markovian temporal network model derived from $G^{(2)}$ (and thus to a random walk running on the weighted aggregate network) according to Eq. 3 in our Letter. Based on the sequence of eigenvalues $1 = \tilde{\lambda}_1 \geq |\tilde{\lambda}_2| \geq \dots \geq |\tilde{\lambda}_n|$ of $\tilde{\mathbf{T}}^{(2)}$ with corresponding eigenvectors $\tilde{v}_1, \dots, \tilde{v}_n$, a convergence time $\tilde{t}(\epsilon)$ after which total variation distance falls below ϵ can then be derived analogously as:

$$\tilde{t}(\epsilon) = \frac{1}{\ln(|\tilde{\lambda}_2|)} \cdot \left(\ln(\epsilon) - \ln \left(\frac{1}{2} \sum_{j=1}^n |\tilde{a}_2(\tilde{v}_2)_j| \right) \right)$$

A fraction $\mathcal{S}^*(\mathbf{T}^{(2)}, \epsilon)$ that captures the slow-down (or speed-up) of convergence that is due to non-Markovian properties can then be defined based on $t(\epsilon)/\tilde{t}(\epsilon)$:

$$\mathcal{S}^*(\mathbf{T}^{(2)}, \epsilon) := \frac{\ln(|\tilde{\lambda}_2|)}{\ln(|\lambda_2|)} \cdot \frac{\ln(\epsilon) - \ln \left(\frac{1}{2} \sum_{j=1}^n |a_2(v_2)_j| \right)}{\ln(\epsilon) - \ln \left(\frac{1}{2} \sum_{j=1}^n |\tilde{a}_2(\tilde{v}_2)_j| \right)}$$

We then define the proportional slow-down $\mathcal{S}^*(\mathbf{T}^{(2)})$ in the limit of small ϵ (or large k) as

$$\mathcal{S}^*(\mathbf{T}^{(2)}) := \lim_{\epsilon \rightarrow 0} \left(\mathcal{S}^*(\mathbf{T}^{(2)}, \epsilon) \right) = \frac{\ln(|\tilde{\lambda}_2|)}{\ln(|\lambda_2|)}. \quad (\text{S4})$$

We remark, that this slow-down is due to the difference in the spectral gap of $\mathbf{T}^{(2)}$ as compared to the null-model $\tilde{\mathbf{T}}^{(2)}$ derived from the weighted aggregate network corresponding to both $\mathbf{T}^{(2)}$ and $\tilde{\mathbf{T}}^{(2)}$. The prediction $\mathcal{S}^*(\mathbf{T}^{(2)})$ holds for sufficiently large k or - equivalently - for a sufficiently small total variation distance ϵ . Furthermore, we assumed that $\tilde{\mathbf{T}}^{(2)}$ is primitive and that λ_2 is non-degenerate.

If the spectral gap $|\tilde{\lambda}_2|$ of the second-order network corresponding to the Markovian temporal network is larger than the gap $|\lambda_2|$ corresponding to a non-Markovian case, $\mathcal{S}^*(\mathbf{T}^{(2)}) > 1$. In this case, the *conductance* of $\tilde{G}^{(2)}$ is larger than that of $G^{(2)}$ and the non-Markovian properties slow down random walk convergence. If - on the other hand - $|\tilde{\lambda}_2|$ is smaller than $|\lambda_2|$, the conductance of $\tilde{G}^{(2)}$ is smaller than that of $G^{(2)}$. In this case $\mathcal{S}^*(\mathbf{T}^{(2)}) < 1$, meaning that the non-Markovian properties of a temporal network speed up random walk convergence.

We finally note that for $|\lambda_2| = |\lambda_3|$, a similar slow-down ratio can be derived for the chi-square distance based on the upper bounds on the second-largest eigenvalues for general directed networks with arbitrary eigenvalue spectra following the arguments put forth in [25]. Based on this approach the prediction would look like

$$S_\chi^*(\mathbf{T}^{(2)}) = \frac{\ln\left(\frac{1}{2}(1 + \operatorname{Re}(\tilde{\lambda}_2))\right)}{\ln\left(\frac{1}{2}(1 + \operatorname{Re}(\lambda_2))\right)},$$

with the eigenvalue sequence of the transition matrix sorted by their real parts, i.e. $\operatorname{Re}(\lambda_1) \geq \operatorname{Re}(\lambda_2) \geq \dots \geq \operatorname{Re}(\lambda_n)$. The prediction $S_\chi^*(\mathbf{T}^{(2)})$ is equal to $S^*\left(\frac{1}{2}(\mathbf{I}_n + \mathbf{T}^{(2)})\right)$ where n is the dimension of $\mathbf{T}^{(2)}$ and \mathbf{I}_n is the corresponding identity matrix. This is equal to applying the prediction S^* to a transition matrix of a lazy random walk with self-loop probability $1/2$. This approach can alleviate periodicity and assure that $|\lambda_2| > |\lambda_3|$ at least for the transition matrix of a lazy random walk.

Details of Model for non-Markovian Temporal Networks A particularly important finding in our Letter is the fact that non-Markovian characteristics can give rise both to a slow-down and speed-up of diffusion dynamics when compared to their static aggregated counterparts. To illustrate this fact, we introduce a simple toy model for temporal networks in which non-Markovian properties can either *inhibit* or *enforce* time-respecting paths across two pronounced communities that are present in the static aggregate network. In our Letter we argue that the presence of order correlations which enforce time-respecting paths across communities is a particularly simple mechanism by which non-Markovian properties in temporal networks can speed up diffusion dynamics. With this we further highlight one possible mechanism by which non-Markovian properties can effectively mitigate the decelerating effect of community structures on diffusion dynamics.

In the following, we formally define our toy model and substantiate our interpretations in the Letter by means of a spectral analysis of the second-order aggregate networks corresponding to different points in the model's parameter space. The model is based on a directed, weighted aggregate network $G^{(1)}$ with two communities, each consisting of a random k -regular graph with n nodes. To interconnect the two communities, we randomly draw edges $e = (v_1, v_2)$ and $e' = (v'_1, v'_2)$ from the two communities respectively, remove e and e' and instead add edges (v_1, v'_1) and (v_2, v'_2) thus maintaining a k -regular aggregate network. We further assign uniform weights ω_1 to all edges, thus obtaining a network as shown in the schematic illustration in Fig. S2 (left panel). For the simulations in the letter, we use $k = 4$ and $n = 50$, thus obtaining a network with 100 nodes and 400 directed edges.

For this first-order network $G^{(1)}$, we construct a second-order network $G^{(2)}$ corresponding to Markovian edge activations as shown in Fig. S2 (right panel). Since $G^{(1)}$ has 400 edges, $G^{(2)}$ has

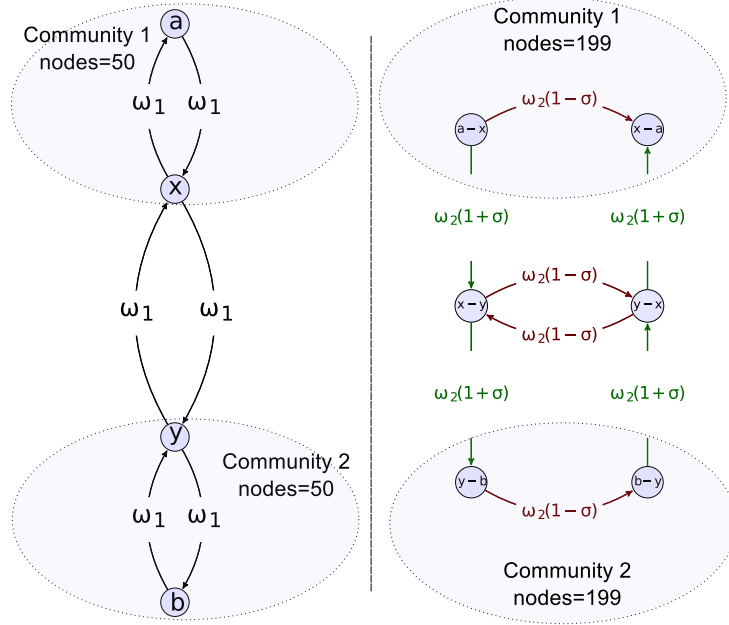


Figure S2: Schematic representation of our model for non-Markovian temporal networks. The first-order aggregate network $G^{(1)}$ (left) consists of two pronounced communities connected by directed inter-community links (x, y) and (y, x) . Weights in the corresponding second-order aggregate network $G^{(2)}$ (right) are changed by means of a parameter σ (right). Positive values for σ enforce two-paths across communities (green) and inhibit two-paths within communities (red).

400 nodes, each corresponding to a directed edge in the first-order network. As weights in the second-order network $G^{(2)}$, we consider a uniform constant ω_2 which corresponds to a Markovian case in which consecutive edge activations are independently drawn. We use the following simple strategy to introduce non-Markovian properties. We first identify all edges (x, y) that interconnect the two communities, i.e. where x is a node in community 1 and y is a node in community 2. For these edges, we then identify two nodes a, b such that a is a node in community 1 adjacent to x and b is a node in community 2 adjacent to node y . The basic idea of the model is to change the weights of those two-paths that involve edges $(a, x), (x, y), (y, x)$ and (x, a) . The statistics of these two-paths is captured by the weights of edges connecting nodes $(a, x), (x, y), (x, a), (a, x)$ in the second-order network (see Fig. S2 (right panel)).

Based on a parameter $\sigma \in (-1, 1)$, the weights of the second-order edges $(a, x) \rightarrow (x, y)$ and $(y, x) \rightarrow (x, a)$ are set to $\omega_2(1 + \sigma)$, while the weights of second-order edges $(a, x) \rightarrow (x, a)$ and $(y, x) \rightarrow (x, y)$ are set to $\omega_2(1 - \sigma)$. Weights of second-order edges including the nodes b and y are adjusted analogously (see Fig. S2 (right panel)). By this means, positive values for σ increase

the weights of two-paths *across communities* at the expense of two-paths *within communities*. Negative values for σ increase the weights of two-paths *within communities* at the expense of two-paths *across communities*. A value of $\sigma = 0$ yields a second-order aggregate network with uniform weights ω_2 which - by construction - corresponds to a Markovian case.

For $\sigma \neq 0$, the above procedure leads to transition matrices $\mathbf{T}^{(2)} \neq \tilde{\mathbf{T}}^{(2)}$ which are however consistent with the same weighted aggregate network $G^{(1)}$. This can be confirmed by checking that for all $\sigma \in (-1, 1)$, the stationary activation frequencies of edges captured by the leading eigenvector π of $\mathbf{T}^{(2)}$ is the same. The change of second-order weights by our model imply

$$\begin{aligned} T_{(a,x)(x,y)}^{(2)} &= \omega_2(1 + \sigma), & T_{(y,x)(x,a)}^{(2)} &= \omega_2(1 + \sigma), \\ T_{(a,x)(x,a)}^{(2)} &= \omega_2(1 - \sigma), & T_{(y,x)(x,y)}^{(2)} &= \omega_2(1 - \sigma). \end{aligned}$$

Since the j -th component of the stationary distribution of the second-order network is given by $\pi_j = \sum_i \pi_i T_{ij}^{(2)}$ the changes above only influence entries $\pi_{(x,a)}$ and $\pi_{(x,y)}$ in the leading eigenvector of $\mathbf{T}^{(2)}$. Let $\tilde{\pi} = \tilde{\pi} \tilde{\mathbf{T}}^{(2)}$ and $\pi = \pi \mathbf{T}^{(2)}$. Then for $\pi_{(x,a)}$ we can write

$$\begin{aligned} \pi_{(x,a)} &= \sum_i \pi_{(i,x)} T_{(i,x)(x,a)}^{(2)} \\ &= \sum_{i \neq a, y} \left(\pi_{(i,x)} T_{(i,x)(x,a)}^{(2)} \right) \\ &\quad + \pi_{(a,x)} T_{(a,x)(x,a)}^{(2)} + \pi_{(y,x)} T_{(y,x)(x,a)}^{(2)}. \end{aligned}$$

Recall that our transformations only change the entries for (x, a) and (x, y) therefore it holds that $\pi_{(i,x)} = \tilde{\pi}_{(i,x)}$ for all i . This yields

$$\begin{aligned} \pi_{(x,a)} &= \sum_{i \neq a, y} \left(\tilde{\pi}_{(i,x)} T_{(i,x)(x,a)}^{(2)} \right) \\ &\quad + \tilde{\pi}_{(a,x)} T_{(a,x)(x,a)}^{(2)} + \tilde{\pi}_{(y,x)} T_{(y,x)(x,a)}^{(2)}. \end{aligned}$$

Further we can plug in the definitions for $\mathbf{T}^{(2)}$ from above and also use that $T_{(i,x)(x,a)}^{(2)} = \tilde{T}_{(i,x)(x,a)}^{(2)}$ for all $i \notin \{a, y\}$.

$$\begin{aligned} \pi_{(x,a)} &= \sum_{i \neq a, y} \left(\tilde{\pi}_{(i,x)} \tilde{T}_{(i,x)(x,a)}^{(2)} \right) + && \tilde{\pi}_{(a,x)} \omega_2 (1 - \sigma) \\ & & + && \tilde{\pi}_{(y,x)} \omega_2 (1 + \sigma) \\ &= \sum_{i \neq a, y} \left(\tilde{\pi}_{(i,x)} \tilde{T}_{(i,x)(x,a)}^{(2)} \right) + && \tilde{\pi}_{(a,x)} \omega_2 - \tilde{\pi}_{(a,x)} \omega_2 \sigma \\ & & + && \tilde{\pi}_{(y,x)} \omega_2 + \tilde{\pi}_{(y,x)} \omega_2 \sigma. \end{aligned}$$

Since $\tilde{\mathbf{T}}^{(2)}$ is built from a regular graph it holds that $\omega_2 = \tilde{T}_{(i,x)(x,a)}^{(2)}$ for all i . Hence,

$$\begin{aligned}
\pi_{(x,a)} &= \sum_{i \neq a, y} \left(\tilde{\pi}_{(i,x)} \tilde{T}_{(i,x)(x,a)}^{(2)} \right) + \tilde{\pi}_{(a,x)} \tilde{T}_{(a,x)(x,a)}^{(2)} \\
&\quad - \tilde{\pi}_{(a,x)} \omega_2 \sigma + \tilde{\pi}_{(y,x)} \tilde{T}_{(y,x)(x,a)}^{(2)} + \tilde{\pi}_{(y,x)} \omega_2 \sigma \\
&= \sum_i \left(\tilde{\pi}_{(i,x)} \tilde{T}_{(i,x)(x,a)}^{(2)} \right) - \tilde{\pi}_{(a,x)} \omega_2 \sigma + \tilde{\pi}_{(y,x)} \omega_2 \sigma \\
&= \tilde{\pi}_{(x,a)} - \tilde{\pi}_{(a,x)} \omega_2 \sigma + \tilde{\pi}_{(y,x)} \omega_2 \sigma \\
&= \tilde{\pi}_{(x,a)}.
\end{aligned}$$

In the last step we use that the stationary distribution $\tilde{\pi}$ is uniform and thus $\tilde{\pi}_{(a,x)} = \tilde{\pi}_{(y,x)}$. From an analogous argumentation, we can derive $\pi_{(x,y)} = \tilde{\pi}_{(x,y)}$. We thus confirm that $\pi = \tilde{\pi}$ and the stationary distribution is preserved for $\sigma \in (-1, 1)$. We finally refer the reader to a related model for non-Markovian temporal networks, which has been introduced very recently, during the revision of our manuscript [26]. Different from our approach, the model introduced in [26] generates realizations that do not preserve a given weighted aggregate network, which however is the particular focus of our approach.

Spectral Analysis of the Model The results provided in our Letter show that temporal correlations which are not reflected in the first-order aggregate representation of temporal networks can nevertheless slow-down or speed-up diffusion dynamics. Our interpretation of this effect is that temporal correlations can either mitigate or enforce the decelerating effect of community structures on diffusion dynamics [23]. In the following, we substantiate this interpretation. By means of a spectral analysis of the second-order networks resulting from our model, we show that non-Markovian properties indeed mitigate or enforce community structures in the causal topology of time-respecting paths.

We first define a Laplacian matrix for the second-order aggregate network based on the matrix $\mathbf{T}^{(2)}$ as

$$\mathcal{L} = \mathbf{I}_n - \mathbf{T}^{(2)}$$

where \mathbf{I}_n is the n -dimensional identity matrix. This allows us to study the *algebraic connectivity* as well as the *Fiedler vector* of the weighted second-order networks for different points in our model's parameter space. Algebraic connectivity is defined as the second-largest eigenvalue $\lambda_2(\mathcal{L})$ of the Laplacian \mathcal{L} . Its magnitude has been shown to reflect how "well-connected" a network is and whether its topology exhibits *small cuts* [27, 28].

Fig. S3 shows the algebraic connectivity of second-order aggregate networks $G^{(2)}$ for different points σ in the parameter space of our toy model. The results confirm that positive values for

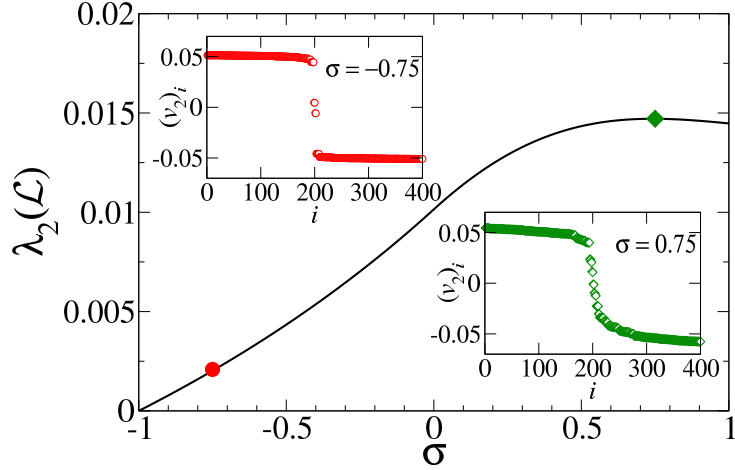


Figure S3: Algebraic connectivity $\lambda_2(\mathcal{L})$ of the weighted second-order aggregate network for different parameters σ our model ($n = 50$) of non-Markovian temporal networks. Insets show the Fiedler vector for two realizations of the model with $\sigma = -0.75$ (red) and $\sigma = 0.75$ (green) corresponding to two cases where two-paths across communities are inhibited and enforced respectively.

σ indeed result in better connected second-order networks compared to a “Markovian” case. On the other hand, negative values for σ result in second-order networks with smaller algebraic connectivity.

The Fiedler vector is the eigenvector $v_2(\mathcal{L})$ corresponding to the second-largest eigenvalue $\lambda_2(\mathcal{L})$. The distribution of the entries of $v_2(\mathcal{L})$ is related to the existence of communities and it is thus frequently used for divisive spectral partitioning of networks [29]. The insets in Fig. S3 show the entries $(v_2)_i$ of the Fiedler vector. For $\sigma = -0.75$, the strong community structure in the second-order network shows up as two separate value ranges with different signs, while the two entries close to zero represent edges that interconnect communities. Apart from the larger algebraic connectivity, the distribution of entries in the Fiedler vector for $\sigma = 0.75$ shows that the separation between communities is less pronounced.

References

- [1] Martina Morris and Mirjam Kretzschmar. Concurrent partnerships and transmission dynamics in networks. *Social Networks*, 17(3&A54):299 – 318, 1995.
- [2] José Luis Iribarren and Esteban Moro. Impact of human activity patterns on the dynamics of information diffusion. *Phys. Rev. Lett.*, 103:038702, Jul 2009.
- [3] M. Karsai, M. Kivela, R. K. Pan, K. Kaski, J. Kertész, A.-L. Barabási, and J. Saramäki. Small but slow world: How network topology and burstiness slow down spreading. *Phys. Rev. E*, 83:025102, February 2011.
- [4] Luis E. C. Rocha, Fredrik Liljeros, and Petter Holme. Simulated epidemics in an empirical spatiotemporal network of 50,185 sexual contacts. *PLoS Comp. Biol.*, 7(3):e1001109, 03 2011.
- [5] Nicola Perra, Andrea Baronchelli, Delia Mocanu, Bruno Goncalves, Romualdo Pastor-Satorras, and Alessandro Vespignani. Random walks and search in time-varying networks. *Phys. Rev. Lett.*, 109:238701, Dec 2012.
- [6] Michele Starnini, Andrea Baronchelli, Alain Barrat, and Romualdo Pastor-Satorras. Random walks on temporal networks. *Phys. Rev. E*, 85:056115, May 2012.
- [7] Till Hoffmann, Mason A. Porter, and Renaud Lambiotte. Random walks on stochastic temporal networks. In Petter Holme and Jari Saramäki, editors, *Temporal Networks, Understanding Complex Systems*, pages 295–313. Springer Berlin Heidelberg, 2013.
- [8] Naoki Masuda, Konstantin Klemm, and Victor M. Eguiluz. Temporal networks: Slowing down diffusion by long lasting interactions. *Phys. Rev. Lett.*, 111:188701, Oct 2013.
- [9] David Kempe, Jon Kleinberg, and Amit Kumar. Connectivity and inference problems for temporal networks. *Journal of Computer and System Sciences*, 64(4):820 – 842, 2002.
- [10] Vassilis Kostakos. Temporal graphs. *Physica A: Statistical Mechanics and its Applications*, 388(6):1007 – 1023, 2009.
- [11] René Pfitzner, Ingo Scholtes, Antonios Garas, Claudio J. Tessone, and Frank Schweitzer. Betweenness preference: Quantifying correlations in the topological dynamics of temporal networks. *Phys. Rev. Lett.*, 110:198701, May 2013.
- [12] Hartmut H. K. Lentz, Thomas Selhorst, and Igor M. Sokolov. Unfolding accessibility provides a macroscopic approach to temporal networks. *Phys. Rev. Lett.*, 110:118701, Mar 2013.

- [13] M. Rosvall, A. V. Esquivel, A. Lancichinetti, J. D. West, and R. Lambiotte. Networks with Memory. *ArXiv e-prints*, May 2013.
- [14] Lauri Kovanen, Kimmo Kaski, János Kertész, and Jari Saramäki. Temporal motifs reveal homophily, gender-specific patterns and group talk in mobile communication networks. *ArXiv e-prints*, pages 1–8, February 2013.
- [15] Petter Holme and Jari Saramäki. Temporal networks. *Phys. Rep.*, 519(3):97 – 125, 2012.
- [16] Laszlo Lovász. Random walks on graphs: a survey. In *Combinatorics, Paul Erdős is Eighty (Volume 2), Keszthely (Hungary)*, pages 1–46, 1993.
- [17] Philippe Blanchard and Dimitri Volchenkov. *Random Walks and Diffusions on Graphs and Databases*. Springer Berlin Heidelberg, 2011.
- [18] Jae Dong Noh and Heiko Rieger. Random walks on complex networks. *Phys. Rev. Lett.*, 92:118701, Mar 2004.
- [19] Jeffrey S. Rosenthal. Convergence rates for markov chains. *SIAM Review*, 37(3):pp. 387–405, 1995.
- [20] Benjamin Blonder and Anna Dornhaus. Time-ordered networks reveal limitations to information flow in ant colonies. *PLoS ONE*, 6(5):e20298, 05 2011.
- [21] Nathan Eagle and Alex (Sandy) Pentland. Reality mining: sensing complex social systems. *Personal Ubiquitous Comput.*, 10(4):255–268, March 2006.
- [22] Kun Zhao, Márton Karsai, and Ginestra Bianconi. Entropy of dynamical social networks. *PLoS ONE*, 6(12):e28116, 12 2011.
- [23] Marcel Salathé and James H. Jones. Dynamics and control of diseases in networks with community structure. *PLoS Comput Biol*, 6(4):e1000736, 04 2010.
- [24] R. Penrose. A generalized inverse for matrices. *Mathematical Proceedings of the Cambridge Philosophical Society*, 51:406–413, 7 1955.
- [25] Fan Chung. Laplacians and the cheeger inequality for directed graphs. *Annals of Combinatorics*, 9:1–19, 2005.
- [26] R. Lambiotte, V. Salnikov, and M. Rosvall. Effect of Memory on the Dynamics of Random Walks on Networks. *ArXiv e-prints*, January 2014.
- [27] Miroslav Fiedler. Algebraic connectivity of graphs. *Czechoslovak Mathematical Journal*, 23(98), 1973.

- [28] Chai Wah Wu. Algebraic connectivity of directed graphs. *Linear and Multilinear Algebra*, 53(3), 2005.
- [29] Alex Pothén, Horst D. Simon, and Kan-Pu Liou. Partitioning sparse matrices with eigenvectors of graphs. *SIAM J. Matrix Anal. Appl.*, 11(3):430–452, May 1990.